UNCERTAINTY ANALYSIS OF ADIABATIC WALL TEMPERATURE MEASUREMENTS IN TURBINE EXPERIMENTS

S. Lavagnoli, C. De Maesschalck, G. Paniagua
von Karman Institute for Fluid Dynamics, Rhode Saint Genèse, Brussels, Belgium

ABSTRACT

During engine service, turbine components are vulnerable to mechanical failures due to large thermal loads. In addition to the heat flux variations during the transients in an engine cycle, high-frequency unsteadiness occurs at every rotor passage with varying amplitudes originating from complex blade row interactions. The heat transfer is therefore time-dependent due to temporal variations in both the convective heat transfer coefficient as well as in the flow recovery temperature caused by the unsteady work processes within the rotor over tip region. It is apparent that the measurement of heat flux alone is not sufficient to elucidate the physical origin of the heat transfer variations, which in turn are the boundary conditions to design the cooling schemes. Hence, the accurate measurement of the adiabatic wall temperature and the adiabatic local convective coefficient becomes essential to ensure a correct thermal assessment of any turbine hardware.

This paper illustrates different approaches to estimate the relevant flow parameters that drive the heat transfer based on transient turbine experiments. The work presents a detailed uncertainty analysis associated with the determination of the adiabatic wall temperature and the adiabatic convective heat transfer coefficient based on a multi-test strategy and the use of surface temperature measurements. The present study allows experimental and numerical specialists quantifying the error in the measured or calculated local gas temperature and convective heat transfer coefficient. Conducting such analysis prior to any experimental or numerical campaign will serve to minimize the test uncertainty in adiabatic wall temperature as a function of: turbine operating conditions; wall to gas temperature ratios; heat transfer uncertainty levels; number of experiments.

NOMENCLATURE

i	=	Current intensity [A]
h	=	Heat transfer coefficient [W/m²/K]
n	=	Power law exponent (cfr.eq. (2))
$f, \Delta f$	=	Frequency, amplifier bandwidth [Hz]
k	=	Thermal conductivity [W/m/K]
k_b	=	Boltzmann's constant (k_b=1.4E-23 J/K)
Q	=	Heat transfer [W/m²]
q	=	Electron charge (q=1.6E-19 C)
R	=	Resistance [Ω]
RMS	=	Root Mean Square
RSS	=	Root of Sum of Squares
T	=	Temperature [K]
TR	=	Wall-to-gas temperature ratio (T_w/T_{aw})

Greek symbols

ε	=	Noise level
φ	=	Rotor phase [-]
σ	=	Uncertainty (at 95% confidence level)
$\sqrt{\rho c k}$	=	Thermal product [J/m^2/K/s$^{0.5}$]

Subscripts

0	=	Absolute, reference
aw	=	Adiabatic wall
g	=	Gauge
R	=	Coefficient from voltage-resistance calibration
T	=	Coefficient from resistance-temperature calibration
w	=	wall

INTRODUCTION

The understanding of the heat transfer processes is fundamental to design the cooling strategy and predict the life of gas turbine components. Designers need to rely on a robust invariant descriptor of the heat transfer process to estimate metal surface temperatures and thermal gradients [1]. The selection of an appropriate definition of the convective heat transfer coefficient, independent of the thermal boundary conditions, is vital in a high-pressure turbine environment where the airfoils undergo temperature variations due to combustor-generated distortions, viscous effects, cooling and unsteady work exchange across the flow path. The use of convective heat transfer coefficients based on a constant reference temperature undoubtedly leads to erroneous results since such characterization is not independent to local changes of the driving temperature [2, 3].

In 1990 Anderson and Moffat [4] proposed the use of the adiabatic heat transfer coefficient (h_{aw}) and the adiabatic wall temperature (T_{aw}) to

characterize the thermal convection in situations with changing fluid temperatures. It was argued that the h_{aw} parameter, based on the local driving temperature T_{aw}, would be an exclusive function of the aerodynamics and hardware geometry. In several experimental and numerical investigations the local values of heat transfer convective coefficient and T_{aw} are determined from distinct flow solutions at different surface temperature [5], [6]. Experimentalists applied this methodology on turbine hardware tested at engine-scaled conditions in warm wind tunnels performing series of repeated experiments run at different wall temperatures ([7], [8], [9]) or by varying the gas-to-wall temperature ratio during one single test ([10], [11]).

The present research examines the impact of the selected convective heat transfer cooling law, wall heat transfer measurements error levels, ranges of wall-to-gas temperature ratios and number of multiple experiments on the final uncertainty in adiabatic wall temperature and convective heat transfer coefficients for typical engine-representative turbine experiments.

MEASUREMENT OF THE HEAT TRANSFER PARAMETERS

The determination of the adiabatic wall temperature is based on the measurement of the heat flux at a number of surface wall temperatures. Experimentally, this requires multiple tests to be run in a transient facility where the local wall temperature is adjusted to different levels prior to a test. Alternatively, a sufficiently long blow-down phase can cause a suitable substrate temperature rise in order to extract the T_{aw} and h_{aw}. Different techniques can be applied to heat up or cool the gauge substrate using heating elements, such as flexible/insertion heaters, electrical heaters, Peltier heat pumps [8].

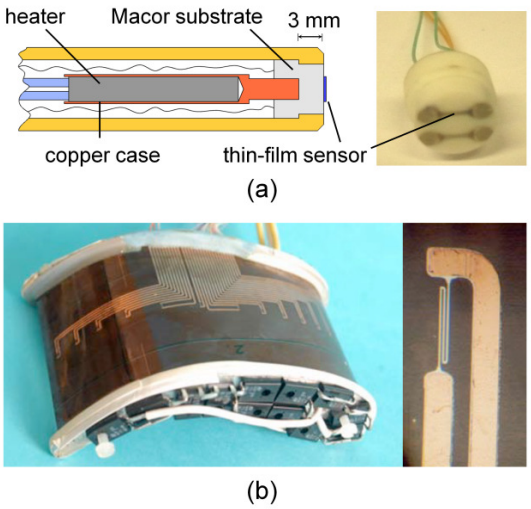

Fig. 1: Compact probe with single-layer thin films on a Macor substrate (a), Vane instrumented with double-layered gauges (b).

Fig. 1 shows examples of research articles instrumented with thin-film sensors and equipped with heating devices that permit the adjustment of the substrate temperature: a compact casing probe with single-layered thin film gauges including a miniature cartridge heater [7], and a stator vane airfoil surrounded by double-layered gauges and a set of electrical resistances glued at the airfoil top and bottom surfaces [12].

An example of the procedure for the adiabatic wall temperature data reduction is given in Fig. 2, [7]. In this particular case, the low- and high-frequency components of the wall temperature were monitored during a turbine test at the rotor casing. From the voltage traces, the original thin-film resistance values can be converted into temperature signals through the calibration law. Several approaches are available to extract the time-varying heat flux from surface temperature measurements. Under the assumption of 1D semi-infinite heat transfer, Fourier transform or impulse response methods can be applied [13]. Direct numerical solution of the unsteady conduction equations using a Crank-Nicholson discretization scheme allows accounting for multilayered substrates [14]. Finite element solvers can deal with complex 2D/3D substrate geometries with temperature-dependent thermal properties [15].

The measured time-averaged wall temperature and the corresponding time-average heat flux of each turbine test are averaged over a time window of about 50-100 ms (Fig. 2-left side). The zero-mean unsteady wall temperature signal is first ensemble-averaged to isolate the deterministic temperature fluctuations, periodic with the rotor blade passage.

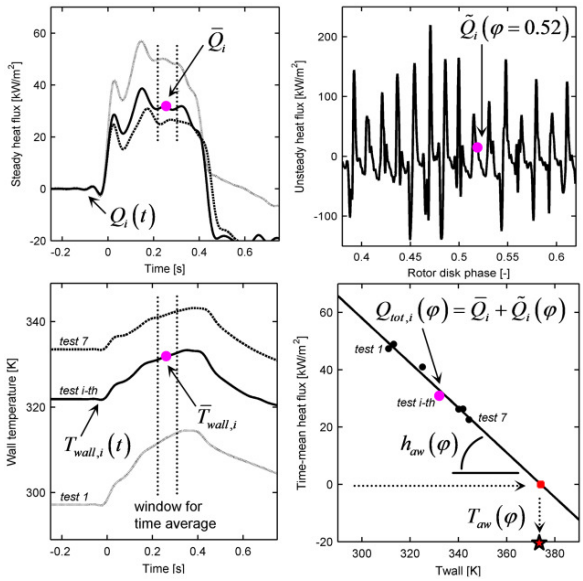

Fig. 2: Methodology for retrieving heat transfer and adiabatic wall temperature from wall temperature measurements [7]

The phase-locked wall temperature trace yields the unsteady time-periodic wall heat flux. The mean heat flux value is then added to the time-periodic heat flux to reconstruct the total time-resolved heat flux over a blade passage event. At each rotor phase value, the variation in heat flux with wall temperature is used to retrieve the adiabatic wall temperature (Fig. 2-lower right).

In convective heat transfer problems, the heat flux is usually expressed with the conventional Newton's cooling law using the concept of adiabatic wall temperature as the driving temperature [1]:

$$\dot{Q}_w = h_{aw}\left(T_{aw} - T_w\right) \qquad \text{eq. (1)}$$

where the adiabatic wall temperature is determined as the wall temperature that yields zero heat flux. The local convective heat transfer coefficient is the gradient of the linear regression line that fits the experimental data (Q_w, T_w) as prescribed in eq. (1). This procedure assumes that a linear relationship exists between the measured heat flux and the wall temperature, i.e., the heat transfer coefficient is constant with the local value of the wall temperature. In reality, the fluid properties (viscosity, thermal conductivity, specific heat) are functions of the fluid temperature. Therefore, variations of the wall-to-gas temperature ratio ($TR=T_w/T_{aw}$) lead to alterations of the local fluid properties, and thus to a modification of the boundary layer. Kays et al. [16] documented several correlations to rectify this effect; one of the most used equations is referred to as the temperature ratio method:

$$h\left(T_w\right) = h_{aw}\left(T_w / T_{aw}\right)^n \qquad \text{eq. (2)}$$

The exponent of the power law, n, is based on theoretical and empirical evidence. Kays et al. [16] recommend n=-0.39 for a turbulent boundary layer. Other authors [17] suggest n=-0.25, deduced from a set of numerical and experimental data on a turbulent flat plate. In the present study eq. (2) is used to correct the linear Newton's cooling law. Consequently, the heat transfer data from multiple turbine experiments is modeled according to:

$$\dot{Q}_w = h_{aw}\left(T_w / T_{aw}\right)^n \left(T_{aw} - T_w\right) \qquad \text{eq. (3)}$$

Once the three heat transfer parameters (T_{aw}, h_{aw} and the exponent n) are determined from the experimental data, eq. (2) can be used to establish the actual convective heat transfer coefficient at a particular wall temperature ratio.

HEAT FLUX UNCERTAINTY

The uncertainty analysis is based on the methodology proposed by Coleman and Steele [18], and bias and precision errors are distinguished. All error estimates are given at the 95% confidence level.

Wall temperature. The measured wall temperature T_w is determined from the thin-film gauge voltage through the temperature-resistance calibration of the sensor and the calibration of the conditioning electronics chain. The measurement accuracy can be deducted from the following data reduction equation:

$$T_w = \Delta T_w + T_{w,0} = a_T\left(a_R V_g + b_R\right) + b_T \qquad \text{eq. (4)}$$

The measurement system allows to monitor the absolute wall temperature value ($T_{w,0}$), and the variations in the gauge temperature during the test blow-down (ΔT_w). Errors introduced by the gauge temperature-resistance calibration and the conditioning electronic calibration (voltage-to-resistance relationship) produce bias errors in the wall temperature measurement. Signal noise generates a random uncertainty in the measurement of the sensor voltage (V_g). Errors engendered by the finite thickness of the surface sensor and the non-uniformity of the sensing metallic layer deposition are neglected in this analysis. The quantization error (bias) due to the discrete signal sampling can also be considered negligible. The sensor is assumed to yield repeatable measures and show no hysteresis. The uncertainty of each parameter is reported in Table 1 together with the overall error in the wall temperature measurement.

Typical uncertainties for the temperature-resistance calibration coefficients a_T and b_T are respectively 0.25-0.4% and 1.5-2.5% of the mean value, principally due to temperature non-uniformities within the controlled calibration room (±0.1 K) and the precision of the reference thermometer (±0.1 K). The values of a_R and b_R are calibrated with high precision for each channel of the heat transfer conditioning electronics leading to very low uncertainties in T_w.

The measurement of the output voltage is affected by white noise generated by the conditioning electronics and by the resistance gauge itself. The primary sources of gauge noise are the shot noise and the Johnson noise [19]. The corresponding noise voltages can be evaluated through equations eq. (5) and eq. (6):

$$\sigma_{shot} = R\sqrt{2qi\Delta f} \qquad \text{eq. (5)}$$

$$\sigma_{Johnson} = \sqrt{4\kappa_b TR\Delta f} \qquad \text{eq. (6)}$$

Considering a thin-film resistance of 50 Ω fed by a current of 10 mA and a system bandwidth of 100 kHz, the shot and Johnson noise voltages are 900 nV rms and 300 nV rms respectively. The noise generated by the thin-film leads can be neglected for small wire resistances ($R_{lead} < 0.5$ Ω). The noise generated by the heat transfer amplifier circuitry designed for low-noise applications can typically range between 0.5-2.0 μV rms. Assuming a total RSS noise voltage at the amplifier input of 1.5 μV rms, the output noise voltage is 2.5 mV given a maximum amplifier gain of 64 dB at 100 kHz [20]. Propagation of the random noise voltage into the wall temperature measurement leads to a precision uncertainty in T_w of about 0.1 K rms (20:1). In order to improve the signal-to-noise ratio and reduce the precision error in the wall temperature measurements, digital post-filters and averaging techniques can be used on the raw thin-film signals. A low-pass filter applied to the time-average wall temperature serves to lower the amplitude and the frequency content of the noisy wall temperature fluctuations. Phase-lock averaging of the unsteady wall temperature over the blade passing period substantially attenuates the random signal component. The accuracy on the phase-resolved wall temperature value increases with the square root of the number of samples used in the average (e.g. the number of samples can be increased by increasing the data acquisition sampling rates and by ensemble-averaging over a larger number of rotor blade passages).

For typical experimental conditions, the total uncertainty in $T_{w,0}$ results in relatively high values of about ±2-3 K when the absolute value of the thin-film temperature is directly determined from the temperature-resistance calibration law. The error in the estimation of the intercept b_T (bias error) is the main contributor. However, a number of procedures can be applied to reduce the error on the wall temperature offset: the sensor resistance can be directly measured prior to a test and thus yield a reference value to adjust the gauge calibration; another method consists in monitoring the gauge excitation current as proposed in [21]; a third technique uses the temperature readings from multiple sensors embedded in the substrate (e.g. thermocouples as in Fig. 1a) to correct the wall temperature measurement. Based on the uncertainty associated to these auxiliary measurements, the error in $T_{w,0}$ can be reduced down to ±0.2-0.5 K.

Overall, for a typical turbine experiment, the raw wall temperature measurements are affected by a bias error of ±0.25 K and a random error of ±0.10 K. The precision error can be reduced to ±0.01 K after low-pass filtering at 500 Hz (blowdown transient) and to ±0.002 K for time-resolved wall temperature traces, phase-averaged at the blade passing frequency.

	Source	$\Delta\theta_i$		$\Delta T_{w,i}$ [K]
Bias	a_T	0.40	%mean	0.115
	b_T (T-R calibr.)	2.50	K	2.500
	b_T (corrected)	0.20	K	0.200
	a_R	0.10	%mean	0.030
	b_R	0.50	mΩ	0.015
	ΔV A/D	40.0	μV	0.001
			Tot. BIAS	**0.235**
Random	*ΔV noise*			
	Raw signal	2.50	mV	0.100
	Low-pass filter			**0.010**
	Phase-locked			**0.002**

Table 1: Wall temperature uncertainty (R_g=50 Ω, i=10 mA, Δf=100 kHz, ΔT_w=30 K)

Wall heat flux. The uncertainty in the wall heat flux measurement can be evaluated by means of the following equation:

$$\dot{Q}_w = \sqrt{\rho c k}\,\Delta T_w \sqrt{2\pi f} \qquad \text{eq. (7)}$$

eq. (7) describes the relationship between the heat flux and the wall temperature in the case of periodic mono-dimensional heating through a semi-infinite single-layer substrate. Heat transfer measurements are affected by uncertainties in the measured wall temperature change and in the thermal product of the substrate.

The present uncertainty analysis deals with a single-layer substrate and does not accounts for uncertainties associated to multi-layer or double-side thin-film gauge configurations. A detailed uncertainty analysis for these types of sensor design can be found in the open literature [14], [22]. The effect of the thin-film layer thickness on the flow status can be considered negligible [23]. The data processing technique used to extract the heat flux from the wall temperature time-series is hypothesized to introduce only minor errors into the heat flux value.

Measurements on a Macor ceramic substrate have shown that the uncertainty in the thermal product is typically ±4.0-6.0% (20:1) which appears as a fixed bias error in Q_w. The thermal properties of the substrate are usually assumed to remain constant over the spanned wall temperature range and a fixed value of the thermal product, obtained from a calibration at ambient temperature (T_{ref}=300 K) is used throughout the data reduction procedure. Therefore, variations in the thermal product with temperature introduce a systematic error into the determination of the heat flux. Fig. 3-left shows that the thermal product of Macor drops by 4% when submitted to an increase of temperature of 200 K [24]. Fig. 3-right displays the error in Q_w the article is exposed to a perfect step and the heat flux is determined assuming constant thermal properties evaluated at the reference temperature. The heat flux error is proportional to

the rate of change in thermal product and is nearly 2% when the actual substrate temperature is 80 K larger than the reference temperature. This error can be reduced to less than 1% by considering constant substrate thermal properties evaluated at the initial substrate temperature. Hence, this source of uncertainty can be easily minimized. The error in the temperature-dependent thermal product due to the uncertainty in the absolute wall temperature can be disregarded since the sensitivity of the thermal product to temperature is weak (about 0.03%/K, Fig. 3-left).

The systematic uncertainty in wall temperature generates an error into the heat flux measurements that can be expressed as a fraction of the heat flux value:

$$\varepsilon_{\dot{Q}_w,BIAS} = \frac{\partial \dot{Q}_w}{\partial \Delta T_w}\varepsilon_{T_w} = A\dot{Q}_w \qquad \text{eq. (8)}$$

The wall temperature change in time determines the heat flux, and thus a bias error in the absolute wall temperature does not propagate into Q_w. Propagation of the random uncertainty in T_w into the heat flux can be determined using the methodology of Coleman and Steele applied to equation eq. (7):

$$\varepsilon_{\dot{Q}_w,RAN} = \frac{\partial \dot{Q}_w}{\partial \Delta T_w}\varepsilon_{T_w} = \sqrt{\rho ck}\sqrt{2\pi f}\,\varepsilon_{T_w} \qquad \text{eq. (9)}$$

Equation eq. (9) shows that the precision error in Q_w is proportional to the wall temperature noise level and to the square root of the frequency (f) at which the random noise manifests in the wall temperature signal. Therefore, the random uncertainty in T_w introduces a constant precision error in Q_w. This analysis shows the importance of reducing the amplitude as well as the frequency content of the embedded noise in T_w measurements to minimize the resulting random uncertainty in Q_w. In a typical turbine experiment, the random uncertainty in the total time-resolved heat flux Q_w can be estimated as the sum of the random uncertainties in the time-averaged and in the unsteady heat flux components. Practically, the largest source of uncertainty in Q_w comes from the thermal product and the overall uncertainty is ±6.1%. Table 2 summarizes the contribution of the measured parameters to the wall heat flux uncertainty.

UNCERTAINTY ANALYSIS ON THE HEAT TRANSFER PARAMETERS

Bias error. The determination of the parameters that describe the convective thermal process is based upon the fit of the experimental heat flux and wall temperature data through the use of a model function, described by eq. (3). Therefore, the experimentalist must determine three parameters (T_{aw}, h_{aw} and the exponent n) to accurately assess the convective thermal process. The uncertainty in these measured parameters is influenced by a number of factors: the number of measurement points, the spanned wall temperature range, the errors in heat flux and wall temperature measurements, the repeatability and the stability of the transient test conditions.

	Source	$\Delta\theta_i$		$\Delta Q_{w,i}$ [%]
Bias	$\sqrt{\rho ck}$	6.00	%mean	6.00
	$\Delta(\sqrt{\rho ck})/\Delta T$	1.00	%mean	1.00
	T_w - BIAS	0.12	K	0.25
			Tot. BIAS	**±6.09%**
	ΔT_w *noise*			**$\Delta Q_{w,i}$ [kW/m^2]**
Random	T_w raw	0.1	K	85.0
	T_w *time-average*	0.01	K	**0.85**
	T_w *phase-averaged*	0.001	K	**2.30**
			Tot. RANDOM*	**±2.45**

*Calculated as the RSS of the time-average and phase-average contribution

Table 2: Wall heat flux uncertainty

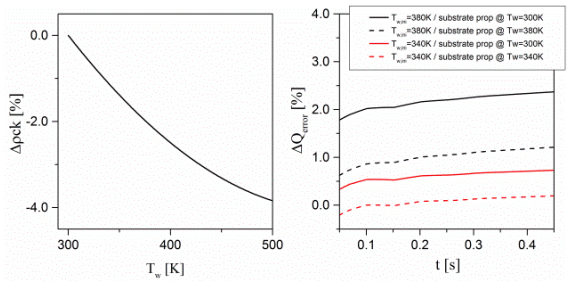

Fig. 3: Thermal product variation with emperature (left); error in heat flux using constant thermal properties for a heat flux step (right).

The propagation of the bias uncertainties in T_w and Q_w into the measurement of T_{aw}, h_{aw}, n was evaluated by calculating the variation in the parameters when the heat flux and wall temperature data points were changed by the corresponding bias error values. Table 3 summarizes the systematic uncertainty in the heat transfer parameters for typical turbine test conditions (h_{aw}=2000 W/m^2/K, T_{aw} =360 K, $T_{w,ref}$=300, n=-0.39).

The bias error in heat flux does not affect T_{aw} and identical conclusion was found by Thorpe et al. considering the Newton's cooling law [21]. The bias error in T_w does propagate through eq. (3) and the T_{aw} is affected by the same error. The bias error in h_{aw} is dominated by the systematic uncertainty in Q_w and the total bias uncertainty in h_{aw} is ±6.1%. It is interesting to note that the bias error in heat flux does not influence the bias uncertainty in the measured exponent n, while the contribution from the bias uncertainty in wall temperature is relatively small. eq. (2) was then used to calculate the bias uncertainty in h_{ref} associated to the bias

errors in T_{aw}, h_{aw} and n using the Coleman and Steele approach. Table 4 lists the estimated uncertainties in h_{ref}. The major contributor to the systematic error in h_{ref} is the uncertainty in h_{aw} and the other sources of error can be neglected.

Source	$\Delta\theta_i$		ΔT_{aw} [K]	Δh_{aw} [%]	Δn [-]
T_w	0.235	K	0.235	0.10%	0.004
Q_w	6.1	%mean	0.0	6.09%	0.0
		Total - BIAS	**±0.235**	**±6.09%**	**±0.004**

Table 3: Bias uncertainty in heat transfer parameters

Source	$\Delta\theta_i$		$\Delta h_{aw,ref}$ [%]
T_{aw}	0.235	K	0.03
h_{aw}	6.09	%mean	6.09
n	0.004		**0.17**
		Total - BIAS	**±6.10%**

Table 4: Bias uncertainty in reference adiabatic convective coefficient ($T_{w,ref}$=300 K)

Random error. The measurement of the heat transfer parameters is also affected by random uncertainties introduced by precision errors in the measured quantities (instrumentation) and repeatability levels in the experimental conditions (test rig). The variations in run conditions are assumed to generate normally distributed random changes in the aerothermal flow field established in the turbine hardware. In the present work, the factors accounted for the test-to-test variability are the change in turbine inlet total pressure (P_{01}) and total temperature (T_{01}). These variations will engender changes in Reynolds number (change in h_{aw}) and in flow total temperature (local change in T_{aw}). Other factors that influence the reproducibility of the aerothermal flow such as rotor speed, turbine pressure ratio and massflow aree not considered here.

The change in the local h_{aw} and adiabatic wall temperature was evaluated on the turbine casing at the rotor exit plane. A turbine through-flow solver was used to quantify the change in flow parameters caused by typical test-to-test variations in P_{01} and T_{01}. The resulting variation in h_{aw} was estimated using the correlation for a laminar flow over an isothermal plate ($Nu=0.664Re^{1/2}Pr^{1/3}$) based on the updated flow information. For simplicity, the change in local T_{aw} was assumed identical to the change in the local total flow temperature. Eventually, an approximate estimation of the sensitivity of h_{aw} and T_{aw} to the operating conditions is derived.

Typical repeatability levels of the turbine rig provide for P_{01} is ±2.0% (20:1) and for T_{01} of ±3.0 K (20:1). Table 5 summarizes the influence of the inlet boundary conditions variability on the heat transfer parameters. The exponent n was considered here to be independent upon moderate variations in turbine test conditions. The analysis shows that changes in convective heat transfer coefficient are mainly driven by variations in total pressure while the inlet total temperature is the largest contributor to variations in adiabatic wall temperature at the selected turbine location.

Source	σ (20:1)	$\partial h/\partial\theta$	Δh	$\partial T_{aw}/\partial\theta$	ΔT_{aw}
P_{01}	± 2%	0.5	1.00%	30 K/bar	1.35 K
T_{01}	± 3.0 K	0.15	0.09%	1 K/K	3.00 K
		RSS total	**±1.00%**	RSS total	**±3.3 K**

Table 5: Test-to-test repeatability in h_{aw} and T_{aw}

The corresponding variability in test-to-test heat flux is evaluated with the square root of the sum of squares of all the single sources according to the formula:

$$\sigma_{Q_w} = \sqrt{\left(\sigma_h \dot{Q}_w\right)^2 + \left(\sigma_{Taw} h\right)^2 + \left(\varepsilon_{\dot{Q}_w,random}\right)^2} \quad \text{eq. (10)}$$

where $\varepsilon_{Qw,random}$ represents the constant random error in heat flux measurements.

A statistical study was performed based on a Monte Carlo approach to investigate the propagation of random uncertainties into the heat transfer parameters. A large number of artificial heat flux datasets was generated to simulate typical adiabatic wall temperature measurements in the turbine rig. Experiment-like heat flux data were obtained through eq. (3) evaluated at discrete wall temperature for prescribed values of T_{aw}, h_{aw} and n. Normally distributed random noise with a standard deviation equal to σ_{Qw}/1.96 (95% confidence level) was finally added to the nominal heat flux to replicate the heat flux run-to-run variability. The effect of the random error in T_w was judged negligible (typically below ±0.1 K) and was not accounted for in the current analysis. An example of this procedure is illustrated in Fig. 4 where the data points represent the samples measured in multiple turbine tests.

A numerical routine was implemented in Matlab® to perform the fit of the virtual heat flux dataset based on eq. (3) using the Matlab® function *nlinfit*. The non-linear regression yields the value of T_{aw}, h_{aw} and n for each dataset together with the associated confidence intervals (Matlab® function *nlparci*). Accurate estimates of the parameter absolute values and corresponding random uncertainties are obtained by averaging the results from all the simulated datasets. A baseline case was selected to represents realistic wind tunnel conditions: a fixed convective coefficient (h_{aw}=2000 W/m^2/K) and a constant value of the exponent n=-0.39 were considered in the calculations. Typical repeatability levels were

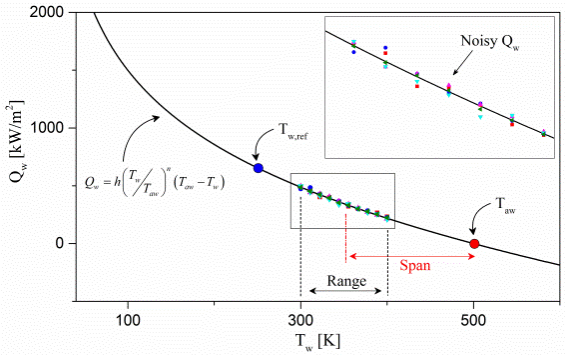

Fig. 4: Simulation of adiabatic wall temperature measurements for uncertainty estimation.

assumed (σ_h=±1.0%, σ_{Taw} =±3.3 K, $\varepsilon_{Qw,random}$=±2.5 kW/m^2). The virtual heat flux was sampled at 20 measurement points spanning a wall temperature range of 60 K (300 K ≤ T_w ≤ 360 K).

The results of the uncertainty analysis are illustrated in Fig. 5. The plots present the difference between the nominal and the "measured" parameter values (that would result from a multi-test strategy) in function of the adiabatic wall temperature. The associated uncertainty levels are represented by the filled colored areas. The absolute value of T_{aw} is accurately determined over a wide range of adiabatic wall temperatures (ΔT_{aw} < 10 for 200 K ≤ T_{aw} ≤ 500 K). The associated random uncertainty remains below ±1.5 K when the set of wall temperatures encompass T_{aw} (interpolation is applied), but it grows very rapidly once the adiabatic wall temperature is found by extrapolation. The absolute reference convective coefficient, $h_{ref}=h_{aw}(T_{w,ref}/T_{aw})^n$, can be accurately retrieved by the experimental procedure, independently of the adiabatic temperature value (Δh_{ref}<3%). The random uncertainty level is bounded between ±5% and ±18% when T_{aw} is comprised within the wall temperature range. However, the random error in convective heat transfer coefficient becomes larger than ±30% when T_{aw}>390 K and T_{aw}<280 K. The bottom graph in Fig. 5 shows that the measurement of the exponent n is affected by a very large precision error (σ_n>±0.75) at any T_{aw} for the investigated experimental conditions. Such an uncertainty level makes quantitative measurements of the exponent n impossible and prevents any attempt to experimentally assess the validity of eq. (3) to model the actual convective thermal processes.

The heat transfer datasets were also fitted using the conventional Newton's cooling law, eq. (1) and results are also reported in Fig. 5. It is interesting to note that the linear regression fit produces more accurate estimates of the true adiabatic wall temperature and convective heat transfer coefficient. Although the non-linear regression would yield close estimations of the parameters' absolute values, the linear fit gives overall more precise estimates of T_{aw} and h_{aw}. Based on the results in Fig. 5, the use of the non-linear fit is adequate to evaluate the convective heat transfer coefficient when T_{aw} falls within the experimental wall temperature range (310 K ≤ T_{aw} ≤ 350 K). The advantage of using the linear model becomes evident when the measurements are carried out under the typical experimental conditions represented by the baseline case. This is due to the fact that a linear regression is generally a more robust tool to fit noisy data which instead introduce large variations in the dependent parameters when a non-linear form is applied.

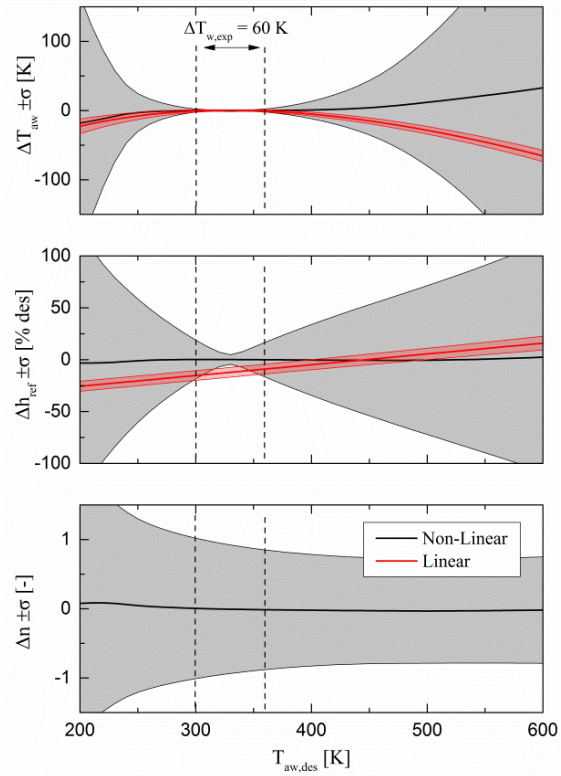

Fig. 5: Absolute value estimate and associated random uncertainty for the three heat transfer parameters as a function the adiabatic wall temperature for non-linear and linear heat transfer models (baseline case).

Impact of the experimental parameters. The number of measurement points and the width of the experimental wall temperature range have a significant influence on the precision uncertainty in T_{aw}, h_{aw}, and n. Fig. 6 displays the variation of the precision error in the three heat transfer parameters as a function of the temperature ratio for three wall temperature ranges (ΔT_w=±20 K, ±30 K, ±40 K) and three different numbers of data points (10, 20, 30).

Increasing the wall temperature range produces significant reductions in the random uncertainty in all the heat transfer parameters. As an example, for measurements at a temperature ratio TR=0.60, the random error drops by 5 K in T_{aw}, 12% in h_{aw} and

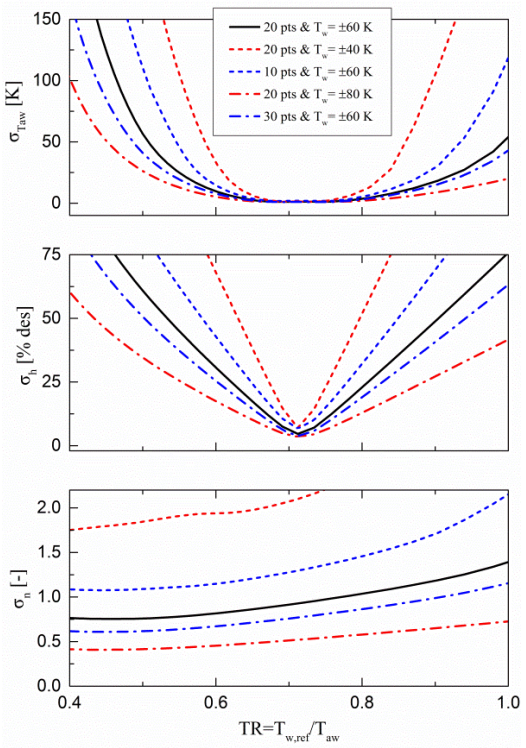

Fig. 6: Random uncertainty in the heat transfer parameters in function of temperature ratio, number of measurement points and wall temperature range (black line is the baseline case).

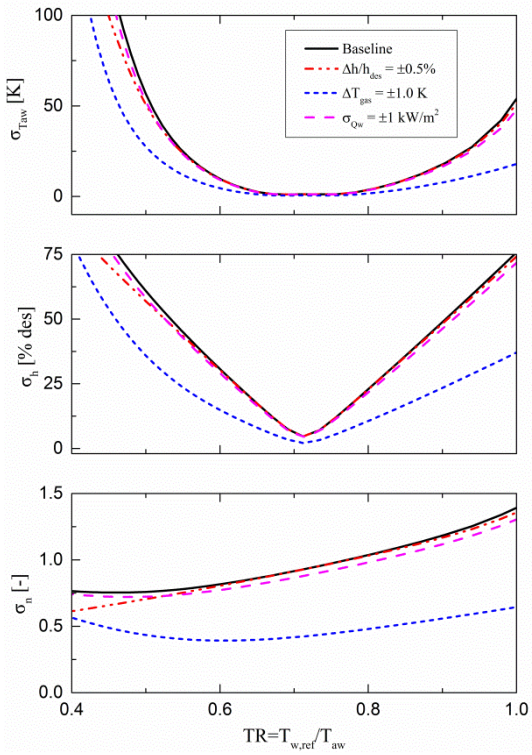

Fig. 7: Random uncertainty in the heat transfer parameters in function of temperature ratio, test-to-test repeatability levels, and instrumentation error.

0.4 in the exponent n when the wall temperature range is broadened from 60 K (baseline case) to 80 K. The error in the experimental data fit reduces with larger numbers of measurement points. The effort to obtain more data points is advantageous to lower the error in T_{aw} when the adiabatic wall temperature falls outside the spanned wall temperature range. On the other hand, a larger number of wind tunnel tests always yields more accurate measurements of $h_{aw,}$ and n.

The impact of repeatability levels in turbine rig aerothermal conditions and of instrumentation accuracy on the uncertainty in $T_{aw,}$ $h_{aw,}$ and n is illustrated in Fig. 7. Under typical experimental conditions (baseline case), a reduction of 50% in the variability of the convective heat transfer process (Δh) or in the heat flux random error (σ_{Qw}) provides only mild improvements in measurement accuracy. On the contrary, a more severe control of the turbine thermal conditions (ΔT_{gas}) leads to a significant reduction in precision uncertainty for all of the three heat transfer parameters.

In order to emphasize the difficulty of measuring with accuracy the exponent n, this uncertainty analysis procedure was used to estimate the minimum requirements in terms of wind tunnel repeatability, instrumentation error and experimental efforts to achieve a precision uncertainty below ±0.05. The parametric study shows that such precision levels can be attained over a large range of temperature ratios by running about 50 turbine experiments which span a wall temperature range of 100 K (275 K ≤ T_w ≤ 375 K), and by simultaneously reducing the test-to-test variability such that Δh=±0.5%, ΔT_{aw}=±0.5 K and σ_{Qw}=1 kW/m^2.

Application to a single turbine test. The uncertainty analysis was also applied to a single test experimental scenario. In this case the heat flux data is collected during the blow-down phase as the substrate temperature will vary in time. A typical heat transfer process during a run in the short-duration facility can be simulated by a gas temperature step where correct aerothermal conditions are sustained for about 300 ms after the initial thermal transient of 100 ms. The blowdown of hot gas over the ceramic substrate will produce a wall temperature change of approximately 30 K as shown in Fig. 8-left. However, only a fraction of the whole temperature change (ΔT_w=10 K) can be effectively used to determine the heat transfer parameters under established aerothermal conditions. As most of the substrate heating occurs in the transient phase, larger wall temperature variations can be obtained with shorter facility start-up times. On the other hand, the single test scenario allows ideally for a more precise control of the turbine operating conditions with respect to repeatability levels associated to a multi-test

strategy. Typical variations in P_{01} and T_{01} during a turbine blowdown are ±0.5% and ±1.0 K respectively. However, it must be noted that, depending on the wind tunnel design, other turbine parameters such as for instance the rotor speed and the rotor tip gap, may show larger variability during a single run compared to a repeated-test approach.

The simulated random uncertainty for a single test is reported in Fig. 8-right. Firstly, the study reveals that the non-linear heat transfer modeling leads to unacceptable errors in the three parameters unless the T_{aw} falls within the narrow available wall temperature range (results not included in here). On the contrary, the use of the Newton's cooling law to fit the data yields accurate estimates for both T_{aw} and h_{aw} (σ_{Taw} < 3 K and σ_{haw} < 2.5%), but significant errors in the parameters' absolute value are expected depending on the measured T_{aw} and the required design temperature ratio.

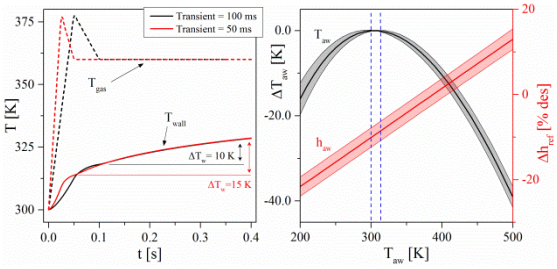

Fig. 8: Simulated heat transfer process for a wind tunnel test (left); random uncertainty in Taw and haw for a single-test scenario using a linear fit (right).

CONCLUSIONS

This work has provided a detailed analysis of the measurement uncertainties associated to the relevant parameters that drive the convective thermal processes based on transient turbine experiments. The paper presents the methodology to determine the adiabatic wall temperature and the adiabatic convective heat transfer coefficient based on a multi-test strategy and the use of surface temperature measurements. A non-linear formulation has been introduced to model the heat transfer process and account for the variation of convective heat transfer coefficient with the wall temperature. This formulation introduces a third parameter (the exponent n in eq. (2)) to be experimentally determined.

A complete uncertainty analysis was carried out where random and bias uncertainties are distinguished. Estimates of the measurement errors in wall temperature and heat flux measurements are provided based on laboratory practice and typical instrumentation performance. The measurement uncertainty in the heat transfer parameters was evaluated based on the instrumentation errors, number of repeated tests and spanned wall temperature range, repeatability levels of turbine operating conditions in a short-duration rig. A Monte Carlo approach was applied to quantify the propagation of the error sources into the final parameters $T_{aw,}$ $h_{aw,}$ and n for multiple-test and single-test measurement strategies. Additionally, a parametric study was performed to assess the influence of each individual error source on the uncertainty attributed to the heat transfer parameters.

The analysis shows that under typical experimental conditions the resulting uncertainty in the parameter n becomes unacceptable (σ_n>0.2), and thus preventing the experimentalist to judge the effective validity of the proposed cooling law form. In such cases, the use of the conventional Newton's cooling law may still be recommended leading to satisfactory levels of uncertainty in the adiabatic wall temperature measurements. Accurate estimates of the exponent n can only be achieved through a tight control of the wind tunnel aerothermal conditions and considerable experimental efforts.

This work provides useful guidelines to design experiments that target the quantification of the local gas temperature and convective heat transfer coefficient in a turbine environment. The uncertainty methodology serves researchers to optimize the use of the available instrumentation resources and wind tunnel performances.

The proposed error analysis represents an effective tool to minimize the uncertainty levels in adiabatic wall temperature measurements and develop more accurate experimental correlations.

ACKNOWLEDGMENTS

The authors would like to thank Jorge Saavedra for some of the heat transfer calculations and acknowledge the contribution of Stefano D'Angelo on the demonstration of the heat flux bias error propagation into the exponent n.

REFERENCES

[1] Moffat, R. J., 1998, "What's New in Convective Heat Transfer?," International Journal of Heat and Fluid Flow, Vol. 19(2), pp. 90-101.

[2] Zhou, X. C. L. J., Aung, K., 2009, "On Selection of Reference Temperature of Heat Transfer Coefficient For Complicated Flows", Heat and Mass Transfer, Vol. 45, pp. 633-643.

[3] Tallman, J. A., Haldeman, C. W., Dunn, M. G., Tolpadi, A. K., Bergholz, R. F., 2009, "Heat Transfer Measurements and Predictions for a Modern, High-Pressure, Transonic Turbine Including Endwalls", Journal of Turbomachinery, Vol. 131(021001).

[4] Anderson, A., Moffat, R. J., 1992, "The Adiabatic Heat Transfer Coefficient and the Superposition Kernel Function: Part II – Modeling Flatpack Data as a Function of Turbulence", Journal of Electronic Packaging, Vol. 114, pp. 22-28.

[5] Shyam, V., Ameri, A., and Chen, J.-P., 2012, "Analysis Of Unsteady Tip And Endwall Heat Transfer In A Highly Loaded Transonic Turbine Stage," Journal of Turbomachinery, Vol. 134(4):041022.

[6] Atkins, N. R., Thorpe, S. J., Ainsworth, R. W., 2012, "Unsteady Effects on Transonic Turbine Blade-Tip Heat Transfer", Journal of Turbomachinery, Vol. 134 (6).

[7] Lavagnoli, S., Paniagua, G., De Maesschalck, C., Yasa, T., 2013, "Analysis of the Unsteady Overtip Casing Heat Transfer in a High Speed Turbine", Journal of Turbomachinery, Vol. 135(3).

[8] Thorpe, S., Yoshino, S. , Ainsworth, R., and Harvey, N., 2004, "An Investigation of the Heat Transfer and Static Pressure on the Casing Wall of an Axial Turbine Operating At Engine Representative Flow Conditions (I): Time-Mean Results," International Journal of Heat and Fluid Flow, 25(6), pp. 933-944.

[9] Polanka, M. D., Anthony, R. J., Bogard, D. G., Reeder, M. F., 2008, "Determination of Cooling Parameters for a High Speed, True Scale, Metallic Turbine Vane Ring", ASME paper GT2008-50281.

[10] Newton, P. J., Lock, G. D., Krishnababu, S. K., Hodson, H. P., Dawes, W. N., Hannis, J., and Whitney, C., 2006, "Heat Transfer and Aerodynamics of Turbine Blade Tips in A Linear Cascade," ASME J. Turbomachinery, Vol. 128(2), pp. 300-309.

[11] Ekkad, S., Ou, S., Rivir, R., 2004, "A Transient Infrared Thermography Method for Simultaneous Film Cooling Effectivenss and Heat Transfer Coefficient Measurements from a Single Test", Journal of Turbomachinery, Vol. 126(4), pp. 597-603.

[12] Pinilla, V., Solano, J. P., Paniagua, G., Anthony, R. J., 2012, "Adiabatic Wall Temperature Evaluation in a High Speed Turbine", Journal of Heat Transfer, Vol. 134(1).

[13] Oldfield, M. L. G., 2008, "Impulse Response Processing of Transient Heat Transfer Gauge Signals", J. Turbomach., Vol. 130(1).

[14] Iliopoulou, V., Denos, R., Billiard, N., and Arts, T., 2004, "Time-Averaged and Time-Resolved Heat Flux Measurements on a Turbine Stator Blade Using Two-Layered Thin-Film Gauges," J. Turbomach., Vol. 126, pp. 570–577.

[15] Solano, J. P., Paniagua, G., 2009, "Novel Two-Dimensional Transient Heat Conduction Calculation in a Cooled Rotor: Ventilation Preheating Blow-Down Flux", Journal of Heat Transfer, Vol. 131(3).

[16] Kays, W. M., Crawford, M. E.,Weigand, B., 2005, "Convective Heat and Mass Transfer", McGraw-Hill Series in Mechanical Engineering.

[17] Fitt, A. D., Forth, C. J. P., Robertson, B. A., Jones, T. V., 1986, "Temperature Ratio Effects in Compressible Turbulent Boundary Layers", Journal of Heat and Mass Transfer, 1986, Vol. 29, pp. 159-164.

[18] Coleman, H. W., Steele, W. G., 2009, "Experimentation, Validation, and Uncertainty Analysis for Engineers" Wiley, 3rd edition, 2009.

[19] Johnson, J., 1928, "Thermal Agitation of Electricity in Conductors", Phys. Rev. 32, 97.

[20] Anthony, R. J., Oldfield, M. L. G., Jones, T. V., and LaGraff, J. E., 1999, "Development of High-Density Arrays of Thin Film Heat Transfer Gauges," Proceedings 5th ASME/JSME Thermal Engineering Joint Conference, San Diego, CA, March 15–19.

[21] Thorpe, S. J. , Yoshino, S., Ainsworth, R. W. , Harvey, N. W., 2004, "Improved Fast-response Heat Transfer Instrumentation For Short-Duration Wind Tunnels." Measurement Science and Technology, 15:1897, 2004.

[22] Anthony, R. J., Clark, J. P., Kennedy, S. W., Finnegan, J. M., 2011, "Flexible Non-Intrusive Heat Flux Instrumentation on the AFRL Research Turbine", ASME paper GT2011-46853

[23] Schultz, D. L., and Jones, T. V., 1973, "Heat Transfer Measurements in Short Duration Facilities," AGARDograph Report No. 165.

[24] MACOR® data sheet at www.corning.com